

LETTER • OPEN ACCESS

## Contrasting climate and carbon-cycle consequences of fossil-fuel use versus deforestation disturbance

To cite this article: K U Jayakrishnan *et al* 2022 *Environ. Res. Lett.* **17** 064020

View the [article online](#) for updates and enhancements.

You may also like

- [Deforestation displaced: trade in forest-risk commodities and the prospects for a global forest transition](#)  
Florence Pendrill, U Martin Persson, Javier Godar *et al.*
- [Effectiveness of regulatory policy in curbing deforestation in a biodiversity hotspot](#)  
B Alexander Simmons, Kerrie A Wilson, Raymundo Marcos-Martinez *et al.*
- [Feedback between drought and deforestation in the Amazon](#)  
Arie Staal, Bernardo M Flores, Ana Paula D Aguiar *et al.*



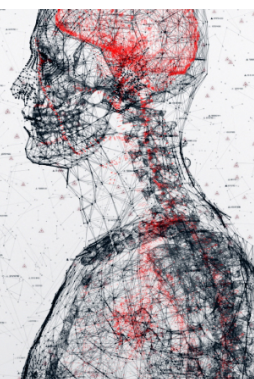
physicsworld

AI in medical physics week

20–24 June 2022

Join live presentations from leading experts  
in the field of AI in medical physics.

[physicsworld.com/medical-physics](https://physicsworld.com/medical-physics)



ENVIRONMENTAL RESEARCH  
LETTERS

## LETTER

## Contrasting climate and carbon-cycle consequences of fossil-fuel use versus deforestation disturbance

## OPEN ACCESS

## RECEIVED

28 October 2021

## REVISED

15 April 2022

## ACCEPTED FOR PUBLICATION

25 April 2022

## PUBLISHED

25 May 2022

Original content from this work may be used under the terms of the [Creative Commons Attribution 4.0 licence](#).

Any further distribution of this work must maintain attribution to the author(s) and the title of the work, journal citation and DOI.

K U Jayakrishnan<sup>1,\*</sup> , Govindasamy Bala<sup>1</sup> , Long Cao<sup>2</sup> and Ken Caldeira<sup>3</sup> <sup>1</sup> Centre for Atmospheric and Oceanic Sciences, Indian Institute of Science, Bangalore 560012, India<sup>2</sup> Department of Earth Sciences, School of Earth Sciences, Zhejiang University, Hangzhou, Zhejiang 310027, People's Republic of China<sup>3</sup> Department of Global Ecology, Carnegie Institution for Science, Stanford, CA 94305, United States of America

\* Author to whom any correspondence should be addressed.

E-mail: [jayakrishnan@iisc.ac.in](mailto:jayakrishnan@iisc.ac.in)**Keywords:** fossil fuel emissions, land use emissions, deforestation, carbon cycleSupplementary material for this article is available [online](#)**Abstract**

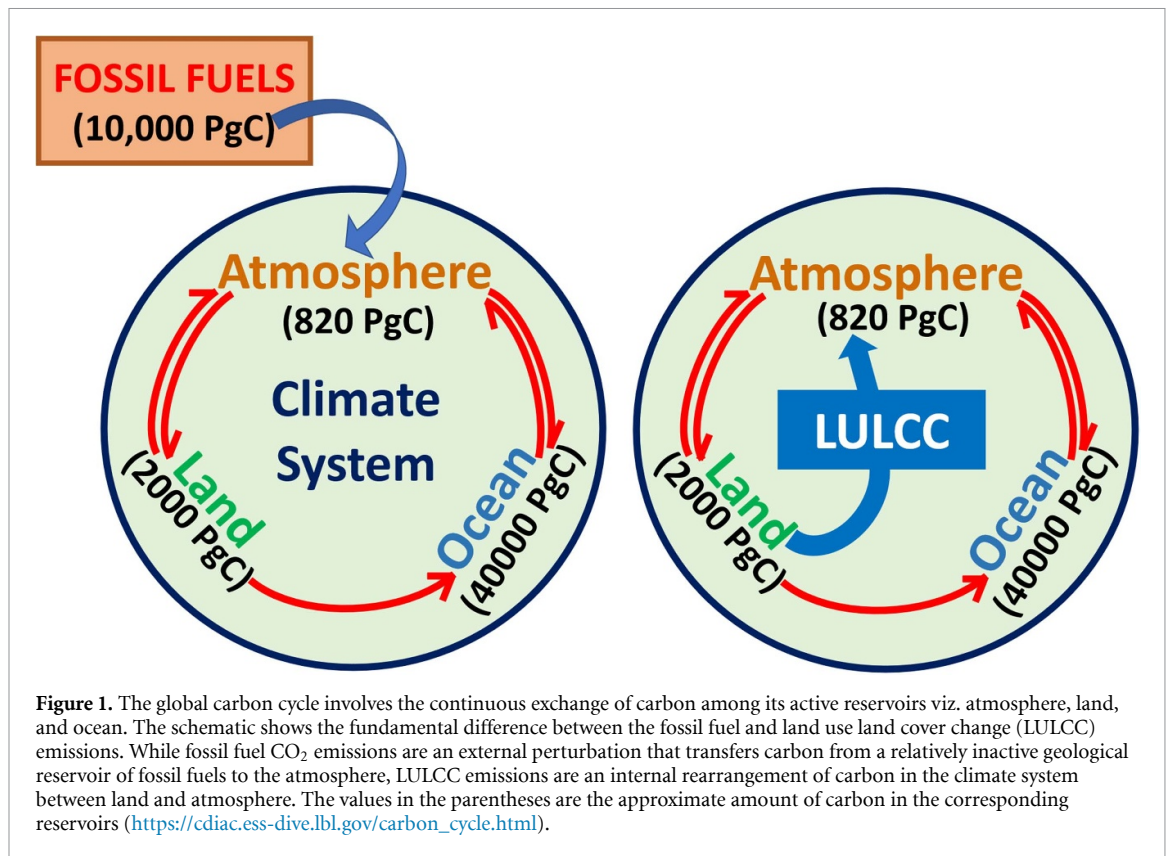
Carbon dioxide emissions from deforestation disturbance (e.g. clear-cutting, forest fires) are in the same units as carbon dioxide emissions from fossil fuels. However, if the forest is allowed to regrow, there is a large difference between climate effects of that forest disturbance and climate effects of fossil CO<sub>2</sub>. In this study, using a set of idealized global climate-carbon model simulations with equal amounts of CO<sub>2</sub> emissions, we show that on century to millennial timescales the response of the climate system to fossil-fuel burning versus deforestation disturbance are vastly different. We performed two 1000 year simulations where we add abrupt emissions of about 600 PgC to the preindustrial state as a consequence of either fossil fuel use or deforestation disturbance with vegetation regrowth. In the fossil fuel simulations, after 1000 years, about 20% of the initial atmospheric CO<sub>2</sub> concentration perturbation remains in the atmosphere and the climate is about 1 °C warmer compared to preindustrial state. In contrast, in the case of deforestation with regrowth, after 1000 years, atmospheric CO<sub>2</sub> concentration returns close to preindustrial values, because deforested land will typically recover its carbon over the decades and centuries in the absence of further human intervention. These results highlight the differences in the degree of long-term commitment associated with fossil-fuel versus deforestation emissions.

**1. Introduction**

In the industrial era, anthropogenic activities have led to an increase in the concentration of atmospheric CO<sub>2</sub> and other greenhouse gases, resulting in global warming. Fossil fuel use and land use and land cover changes (LULCC) are the dominant sources of anthropogenic CO<sub>2</sub> emissions over the past few centuries (Houghton 2007, Le Quéré *et al* 2009, Ciais *et al* 2013). In the beginning of the industrial era (1750–present), carbon emissions from LULCC (mostly deforestation) exceeded those from fossil fuel use. However, fossil fuel emissions increased rapidly and became the primary source of total anthropogenic carbon emissions in the 20th century (Ciais *et al* 2013). During 1750–2011, fossil fuel use and cement production accounted for 375 ± 30 PgC and LULCC accounted for 180 ± 80 PgC of CO<sub>2</sub> emissions into

the atmosphere (Ciais *et al* 2013). In the recent decade (2010–2019), carbon emissions from fossil fuel use and LULCC are estimated as 9.6 ± 0.5 PgC yr<sup>-1</sup> and 1.6 ± 0.7 PgC yr<sup>-1</sup> respectively (Friedlingstein *et al* 2020). Ward *et al* (2014) estimate that, despite the decline in its contribution to total carbon emissions, about 40% of today's radiative forcing could be attributed to LULCC emissions.

Though the radiative effect of CO<sub>2</sub> from these two anthropogenic sources are the same, they differ in the manner they perturb the global carbon cycle and the land surface properties. These fundamental differences may result in distinct climate responses to fossil-fuel and LULCC perturbations. The modern global carbon cycle involves the three active reservoirs of the climate system, viz. atmosphere, ocean, terrestrial biosphere, and the less active geological reservoir of fossil fuels. There is a continuous and relatively rapid



exchange of carbon among the three active reservoirs via processes such as plant photosynthesis, soil respiration, ocean carbon chemistry, carbon fixation by marine organisms, etc. Fossil fuel emissions involve a net transfer of carbon from the geological reservoir to the three active reservoirs of the climate system. In contrast, LULCC emissions involve an internal transfer of carbon from land reservoirs to the atmosphere. Therefore, as shown in figure 1, fossil fuel emissions are an external source of CO<sub>2</sub> to the Earth's rapidly exchanging near-surface carbon pools, while LULCC emissions represent an internal rearrangement of carbon among these pools.

Further, there is a major difference in how the vegetation cover and the land surface characteristics change in fossil fuel and LULCC emission scenarios. Fossil fuel emissions do not involve any direct changes to land surface properties. In contrast, there is a direct change in land cover from forest area to agricultural or pastureland in the case of deforestation, which would result in a decrease in evapotranspiration and an increase in surface albedo. Consequently, the reduction of latent heat fluxes would lead to a warming of the surface (Lean and Rowntree 1993, Bathiany *et al* 2010, Davin and de Noblet-ducouadre 2010), while the increase in albedo from deforestation would have a cooling influence (Govindasamy *et al* 2001, Bala *et al* 2007, Bathiany *et al* 2010, Davin and de Noblet-ducouadre 2010). In addition, removal of forests would result in changes in the concentration of biogenic aerosols, which could have significant

climate consequences (Spracklen *et al* 2008, Petäjä *et al* 2021).

Our focus here is on the relative effects of two emission events, an event in which a forest is converted into CO<sub>2</sub>, after which the forest is allowed to regrow versus fossil fuel emission of CO<sub>2</sub>. There are two motivations for this idealized framing: (a) This is a simple representation analogous to carbon loss from forest-fires or clearcutting for bioenergy. (b) Sustained deforestation requires both a deforestation event and an ongoing effort to maintain the deforested state (on the assumption that a forest would regrow on abandoned land). This study focusses on the deforestation event and not the effort to sustain the deforested state. Therefore, we consider an idealized case in which a forest is cut down and allowed to regrow immediately. In contrast, a recent study (Simmons and Matthews 2016), for assessing the influence of the biophysical effect of deforestation on the linear relationship between global mean surface temperature and cumulative carbon emissions, uses an alternate idealized scenario where the deforested land is maintained after the deforestation event.

The fundamental differences in the nature of fossil fuel and LULCC emissions has been relatively little explored in the literature despite its importance for climate policy development. The goal of this paper is to evaluate how the response of climate system to equal amounts of fossil fuel and LULCC emissions differ, using a set of highly idealized abrupt fossil fuel emissions and global deforestation simulations.

The only type of land-cover change considered here is abrupt global deforestation event (i.e. a global conversion of all plant functional types to croplands). Our simulations are highly stylized and meant to maximize both clarity and signal-to-noise ratios. It may be noted that idealized scenarios are common in the climate modeling literature such as simulations of abrupt doubling or quadrupling of CO<sub>2</sub> (Kravitz *et al* 2015, Eyring *et al* 2016) as they help to derive clear and unambiguous messages that are relevant and useful to policy.

Several previous studies have also used idealized deforestation experiments to gain useful scientific insights, and we list some of them here. Bala *et al* (2007) used several idealized abrupt global deforestation simulations and deforestation in latitude bands to investigate the climate and carbon cycle effects of large scale deforestation, while Davin and de Noblet-Ducoudre (2010) used idealized global deforestation experiments to explore the biogeophysical impact of large-scale deforestation on surface climate. The Land Use Model Intercomparison Project designed to further the understanding of impact of land cover changes on climate uses idealized global deforestation simulation to analyze the effect of biogeophysical and biogeochemical changes on response of the climate to land cover changes (Lawrence *et al* 2016). Tölle *et al* (2017) performed an abrupt deforestation simulation to study the effect of large-scale deforestation on monsoon regions. Devaraju *et al* (2018) used idealized abrupt global and latitude-band deforestation experiments to understand the relative importance of direct and indirect LULCC effects and their teleconnection effects at the biome and global scale, while Boysen *et al* (2020) used idealized deforestation experiments to quantify the biogeophysical and biogeochemical effects of deforestation. Our experiments in this paper belong to this class of idealized simulations.

## 2. Methodology and model description

### 2.1. The University of Victoria (UVic) model

Our simulations use the UVic Earth System Climate Model version 2.9, which is an Earth system Model of Intermediate Complexity (EMIC). EMICs have been developed to fill the gap between coupled Atmosphere-Ocean General Circulation Models and simple conceptual models in the spectrum of climate models (Claussen *et al* 2002) as shown in figure S1 (available online at [stacks.iop.org/ERL/17/064020/mmedia](https://stacks.iop.org/ERL/17/064020/mmedia)). UVic model includes a vertically integrated energy-moisture balance atmospheric model, primitive equation ocean general circulation model with 19 vertical layers, and a dynamic-thermodynamic sea ice model (Weaver *et al* 2001). The terrestrial component of the UVic model consists of Top-down Representation of Interactive Foliage and Flora Including

Dynamics Model together with MOSES land surface scheme (Meissner *et al* 2003). An inorganic ocean carbon cycle is included in the UVic model by following the Ocean Carbon-Cycle Model Intercomparison Project protocols and a marine ecosystem model (Keller *et al* 2012). The sediment processes are represented by an oxic-only model of sediment respiration (Eby *et al* 2009). The UVic model is able to represent the large-scale present-day climate quite well as shown by Weaver *et al* (2001), Skvortsov *et al* (2009) and Eby *et al* (2009). Further details of the UVic model are provided in SI text S1.

### 2.2. Simulations

To assess the differing consequences of fossil-fuel and land-cover change emissions, we spun up the model for 5500 years to an equilibrium state that corresponds to pre-industrial climate with zero agricultural land (croplands and pasture lands), by prescribing zero CO<sub>2</sub> emissions and allowing the atmospheric CO<sub>2</sub> to evolve freely (SI text S2). The evolution of important parameters in this ZERO\_EMIS spinup simulation are shown in figure S2. The near-equilibrium values of global mean SAT and atmospheric CO<sub>2</sub> concentration averaged over the last 100 years of 5500 year simulation are 13.41 °C and 288.51 ppm, respectively, and the trend in global mean SAT over the last 500 years is on the order of 10<sup>-5</sup> °C yr<sup>-1</sup>. Trends of other important parameters over the last 500 years of ZERO\_EMIS are listed in table S1. Starting from the end of the ZERO\_EMIS simulation, an abrupt global deforestation (DEFOR-EST) and an abrupt fossil fuel emission (FOSSIL-FUEL) simulation with equal magnitude of carbon emissions are run for 1000 years.

The vegetation in the UVic model consist of five plant functional types (broadleaf tree, needle leaf tree, C<sub>3</sub> grass, C<sub>4</sub> grass and shrub). A deforestation event in the UVic model is typically performed by prescribing a fraction of the grid cells as agricultural land (croplands and pasturelands). The deforestation event in our simulation involves conversion of existing vegetation into only croplands. When converted to cropland, the fraction of the grid cell that is designated as cropland would initially consist of only bare ground upon which C<sub>3</sub> or C<sub>4</sub> grasses are allowed to grow according to the climatic conditions. In the DEFOREST simulation, all grid cells with vegetation are converted to croplands in the beginning of year 1 by specifying 100% croplands. Thus, at the end of first year the land surface consists of only grass functional types or bare ground. From the second year of DEFOREST case, croplands are set to zero everywhere, allowing vegetation types to evolve dynamically subject to climate conditions and the amount of atmospheric CO<sub>2</sub>. Our simulation is highly idealized as the deforested land may be maintained in deforested condition in the subsequent years in the

real world. However, we are considering only the effect of the deforestation event and not the effort to maintain the deforested land. Therefore, unlike Simmons and Matthews (2016), we allow the vegetation to grow back after the deforestation event in our idealized deforestation simulation. When vegetation is converted to croplands, all the associated carbon is released into the atmosphere immediately, resulting in an emission of 597.38 PgC in the first year of the DEFOREST simulation, and the same amount of carbon is emitted as fossil fuel in the first year of the FOSSIL-FUEL simulation. The emissions from these two sources are set to zero in subsequent years.

### 3. Results

#### 3.1. Evolution of carbon stocks

In the FOSSIL-FUEL case, both land and ocean take up carbon at rapid rates immediately after its release (figures S3(c) and (d)), resulting in a rapid decline of atmospheric carbon stock (figure 2(a)). However, the strength of the oceanic and land sinks decreases rapidly: the oceanic sink decreases from 26.1 PgC yr<sup>-1</sup> to 0.8 PgC yr<sup>-1</sup>, and the land changes from a strong sink of 21.8 PgC yr<sup>-1</sup> to neutral at the end of first 50 years (figures S3(c), (d) and table S2) (The values of the sinks in the first year are excluded for comparison, as the first year involves a large land-atmosphere flux as a result of deforestation disturbance in the DEFOREST case). For the rest of the FOSSIL-FUEL simulation, the ocean acts as a weak sink, and the carbon flux between land and atmosphere is nearly zero (figures S3(e) and (f)). By the end of the millennium, about 54% of the CO<sub>2</sub> pulse is removed by ocean, 24% is taken up by land and 22% remains airborne.

The removal of about 78% of the anthropogenic carbon by oceanic and terrestrial sinks in the FOSSIL-FUEL case lies in the range estimated by previous studies (Archer 2005, Montenegro *et al* 2007, Archer *et al* 2009), which analyzed the fate of anthropogenic carbon on millennial timescales. Though most of the emitted carbon is taken up by ocean and land after 1000 years, since the ocean has become a weak sink and the carbon flux between land and atmosphere is nearly zero (figure S3), the remaining carbon could be removed only by the slow silicate weathering processes, which may take up to several hundred thousand years (Archer 2005). In our simulations, the magnitude of the weathering fluxes is set to be equal to sedimentation flux, keeping the alkalinity of the ocean constant. This simple representation of sediment flux implies no dissolution of carbonate sediments in the long-term carbon cycle.

Similar to the FOSSIL-FUEL case, both land and ocean take up carbon at a rapid rate immediately after the abrupt global deforestation event in the DEFOREST case (figures S3(c) and (d)), and the atmospheric carbon content declines rapidly (figure 2(a)). The rate of decrease in atmospheric CO<sub>2</sub> in the first decade is

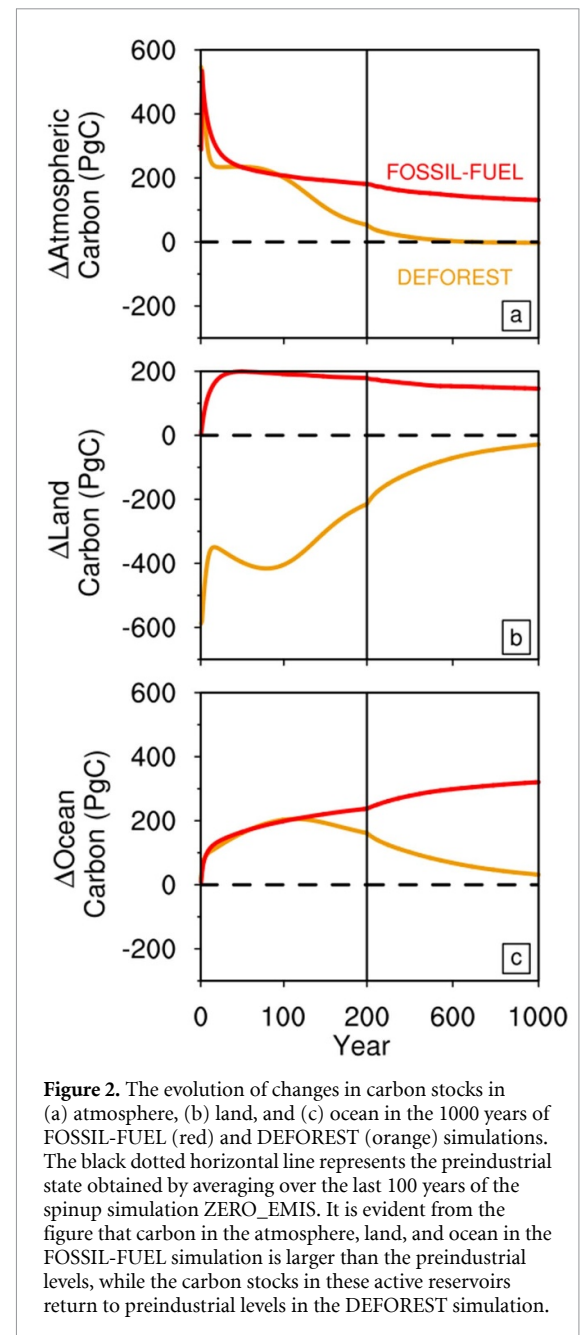
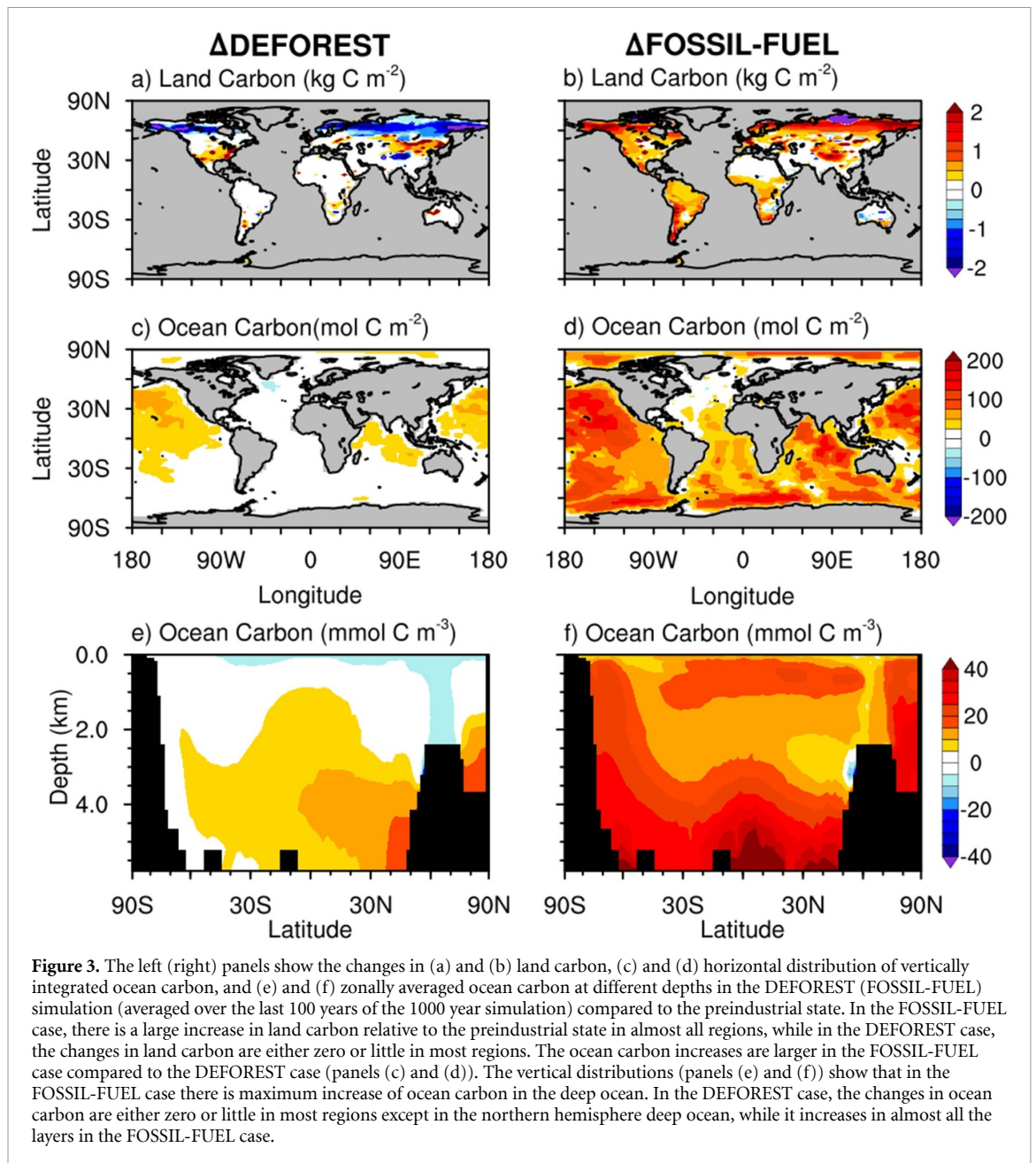


**Figure 2.** The evolution of changes in carbon stocks in (a) atmosphere, (b) land, and (c) ocean in the 1000 years of FOSSIL-FUEL (red) and DEFOREST (orange) simulations. The black dotted horizontal line represents the preindustrial state obtained by averaging over the last 100 years of the spinup simulation ZERO\_EMIS. It is evident from the figure that carbon in the atmosphere, land, and ocean in the FOSSIL-FUEL simulation is larger than the preindustrial levels, while the carbon stocks in these active reservoirs return to preindustrial levels in the DEFOREST simulation.

larger in the DEFOREST case (figure 2(a)) because the regrowth of vegetation results in a stronger terrestrial sink in the DEFOREST case (figure S3(c)). In the DEFOREST case, the strength of the oceanic sink decreases from 20.3 PgC yr<sup>-1</sup> to 1.3 PgC yr<sup>-1</sup> (figure S3(d), table S2), and the land changes from a strong initial sink of 39.5 PgC yr<sup>-1</sup> to a small source of 1.3 PgC yr<sup>-1</sup> by the end of the first 50 years (figure S3(c), table S2). Until year 15, land acts as a net sink because of an abrupt increase in net primary productivity (NPP) compared to the slowly increasing soil respiration (figure S4(b)). After this initial large increase, NPP growth slows down but soil respiration continues to increase (figure S4(b)) because of the warming induced by CO<sub>2</sub> released from deforestation event (as shown later in figure 5) and land becomes a source by year 15.



After year 75, land again becomes a net sink in the DEFOREST case as the amount of atmospheric  $\text{CO}_2$  and warming begin to decline and hence soil respiration decreases (figure S4(b)). The strength of the terrestrial sink increases to  $2.5 \text{ PgC yr}^{-1}$  by year 138 (figure S3(c)), and after that declines and approaches zero as the system reaches near-equilibrium by the end of the simulation (figure S3(e)). After about 115 years, as land takes up more carbon, the atmospheric  $\text{CO}_2$  decreases (see figure 5) and the ocean becomes a weak source (figures S3(d) and (f)) to maintain equilibrium with the atmosphere. The strength of this oceanic source slowly declines to zero by the end of the simulation, after reaching a peak of  $0.7 \text{ PgC yr}^{-1}$  in the year 165 (figure S3(f)).

In the FOSSIL-FUEL case, carbon reservoirs are larger on the land (by  $146.8 \text{ PgC}$ ), in the atmosphere (by  $132.3 \text{ PgC}$ ), and in the ocean (by  $318.4 \text{ PgC}$ ) after 1000 years relative to the preindustrial state, while land and atmosphere lose, respectively,  $32.1$  and  $2.6 \text{ PgC}$ , and ocean gains  $34.7 \text{ PgC}$  in the DEFOREST case relative to the preindustrial state (figure 2, table S3). In the FOSSIL-FUEL case, land carbon increases in most parts of the globe (figure 3(b)), while the changes in land carbon are nearly zero in the DEFOREST case in most regions except in the Northern hemisphere high latitudes where there is a slight decrease in land carbon (figure 3(a)). In the FOSSIL-FUEL case, ocean carbon increases in most regions (figure 3(d)), whereas the ocean carbon in the DEFOREST case increases slightly in some

regions and decreases in other regions with a small net increase (figure 3(c)). In the FOSSIL-FUEL case, the carbon content increases at all levels in the ocean relative to the preindustrial state (figure 3(f)), while in the DEFOREST case, the changes in ocean carbon are either zero or little except in the northern hemisphere deep ocean (figure 3(e)). Note that, though the total ocean carbon content in the DEFOREST case nearly returns to the preindustrial values, the deep ocean carbon has increased slightly. Therefore, it should be emphasized here that, even when the surface climate is restored in the DEFOREST case (section 3.3), deep ocean consequences of the carbon emissions remain on millennial timescales. Similar results have been obtained in simulations of CO<sub>2</sub> removals by carbon dioxide removal technologies (Mathesius *et al* 2015). Thus, while a deforestation-event adds some carbon to the ocean for longer than 1000 years, an equal-sized fossil-fuel emission adds about 9.2 times this amount of carbon. These results illustrate the simple fact that fossil fuel emission is an external perturbation as it adds more carbon to the climate system, while emission from deforestation disturbance is an internal rearrangement of carbon within the climate system.

### 3.2. Changes in land surface characteristics

Figure 4 shows the evolution of the fractional coverage of five plant functional types simulated by the model viz. broadleaf tree, needle leaf tree, C<sub>3</sub> grass, C<sub>4</sub> grass, and shrub, and bare ground in the FOSSIL-FUEL and DEFOREST simulations. In the model, C<sub>3</sub> grass is the dominant vegetation in the preindustrial state. In the FOSSIL-FUEL simulation, the broadleaf tree cover increases a little in the beginning, while the needle leaf tree cover decreases marginally and then increases until the end of the simulations (figure 4(a)). Both the tree type regions have slightly larger fractional coverage by the end of FOSSIL-FUEL simulations relative to the preindustrial state (figure 4(a), table S4). Shrubs and C<sub>3</sub> grasses initially increase and then decrease until the end of simulation, reaching a smaller fractional coverage relative to the preindustrial state (figure 4(a), table S4). The bare ground and C<sub>4</sub> grass areas shrink initially and then increase until the end of simulations, but both have slightly less fractional coverage relative to the preindustrial state (table S4). The increase in forest cover and decrease in fractional coverage of other vegetation types by the end of FOSSIL-FUEL simulation result in a slight decrease in surface albedo compared to the preindustrial state (figure 4(c)).

In the DEFOREST case, C<sub>3</sub> grasses expand the most when vegetation is allowed to grow back after the abrupt global deforestation event (figure 4(b)). The surface albedo in the DEFOREST case shows an abrupt increase because the vegetation is converted to either bare ground or grasslands in the first year (figure 4(c)). After reaching the peak

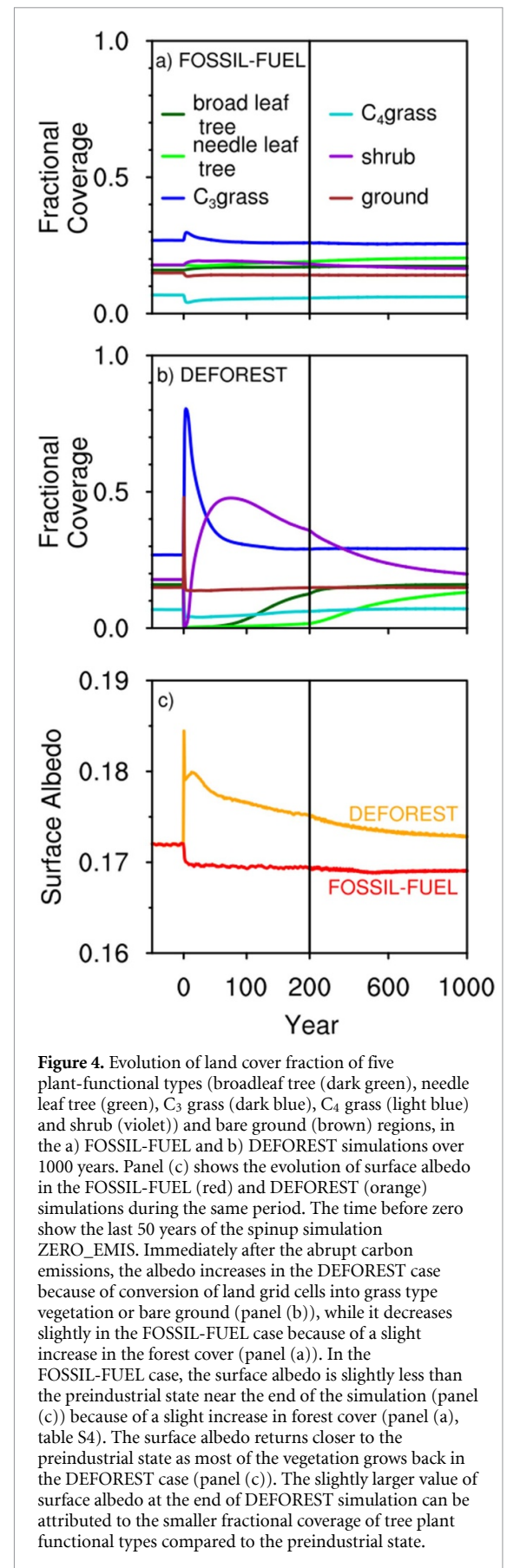


**Figure 4.** Evolution of land cover fraction of five plant-functional types (broadleaf tree (dark green), needle leaf tree (green), C<sub>3</sub> grass (dark blue), C<sub>4</sub> grass (light blue) and shrub (violet)) and bare ground (brown) regions, in the a) FOSSIL-FUEL and b) DEFOREST simulations over 1000 years. Panel (c) shows the evolution of surface albedo in the FOSSIL-FUEL (red) and DEFOREST (orange) simulations during the same period. The time before zero show the last 50 years of the spinup simulation ZERO\_EMIS. Immediately after the abrupt carbon emissions, the albedo increases in the DEFOREST case because of conversion of land grid cells into grass type vegetation or bare ground (panel (b)), while it decreases slightly in the FOSSIL-FUEL case because of a slight increase in the forest cover (panel (a)). In the FOSSIL-FUEL case, the surface albedo is slightly less than the preindustrial state near the end of the simulation (panel (c)) because of a slight increase in forest cover (panel (a), table S4). The surface albedo returns closer to the preindustrial state as most of the vegetation grows back in the DEFOREST case (panel (c)). The slightly larger value of surface albedo at the end of DEFOREST simulation can be attributed to the smaller fractional coverage of tree plant functional types compared to the preindustrial state.

fractional coverage of about 80% by year 4, C<sub>3</sub> grasses start to retreat, while shrubs show rapid expansion and become the dominant vegetation by year 37

(figure 4(b)). Broadleaf trees start to regrow significantly only after year 40, while needle leaf trees take even longer to regrow (figure 4(b)). After year 76, shrubs start retreating, and broadleaf trees expand at faster rates (figure 4(b)). By year 385,  $C_3$  grasses become the dominant vegetation again (figure 4(b)), and all vegetation types except shrub and needle leaf trees reach near preindustrial levels.

For the rest of the DEFOREST simulation, competition is primarily between shrubs and needle leaf trees where the former retreats and later expands, and all other vegetation types show only small changes (figure 4(b)). By 1000 years, shrubs and  $C_3$  grasses (temperate/boreal forests) occupy slightly larger (less) area while other vegetation types approach preindustrial fractional coverage (table S4). The surface albedo at the end of the DEFOREST simulation is slightly larger than preindustrial levels (figure 4(c)) because of a small decrease in the fractional coverage of forests compared to preindustrial coverage (table S4). These results show that the changes in land cover associated with fossil fuel emissions and deforestation disturbance, as well as their impact on land surface properties such as albedo are significantly different, which may result in contrasting effects on the climate system.

### 3.3. Evolution of atmospheric $CO_2$ , surface air temperature (SAT), and surface ocean pH

In the FOSSIL-FUEL case, the atmospheric  $CO_2$  concentration increases by about 62.3 ppm after 1000 years and consequently the climate is warmer by around 1 °C; in the DEFOREST case,  $CO_2$  and SAT values are closer to the original preindustrial values (figure 5, table S3). In addition, the surface ocean pH in the FOSSIL-FUEL case is lower by 0.06, indicating significant ocean acidification in the FOSSIL-FUEL case, while in the DEFOREST case surface ocean pH returns closer to preindustrial value (figure 5, table S3). The abrupt increase in SAT following the emission pulse in the DEFOREST simulation is smaller compared to the FOSSIL-FUEL case, owing to the albedo increase associated with deforestation (figure 4). The competition between the albedo effect from deforestation and the radiative effect of emitted  $CO_2$  results in a fluctuating SAT in the DEFOREST simulation during the first 100 years, while SAT is relatively constant in the FOSSIL-FUEL simulation initially after the abrupt increase (figure 5(b)). The impact of albedo change for conversion from forests to grasslands is larger in the mid-latitudes because the presence of snow cover during winter increases the albedo further through snow-albedo feedback (Snyder *et al* 2004, Bala *et al* 2007, Davin and de Noblet-ducouudre 2010, Devaraju *et al* 2015). Because  $CO_2$  levels in the FOSSIL-FUEL and DEFOREST cases are similar during the first 100 years, most of the differences in temperature response can be attributed to albedo effects in the initial period (figure 5).

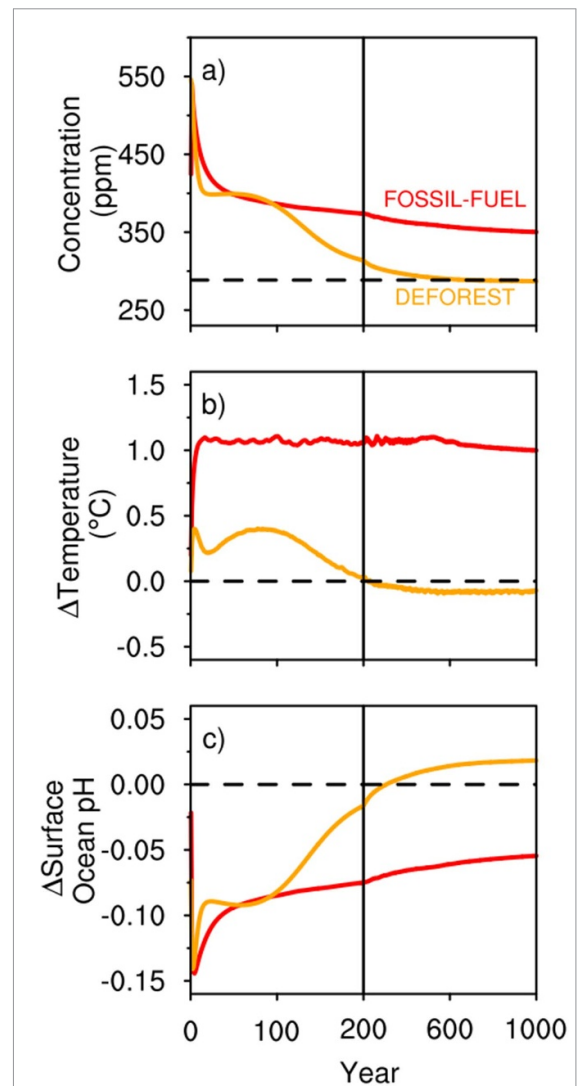


**Figure 5.** Evolution of (a) global mean atmospheric  $CO_2$  concentration, (b) changes in global mean surface air temperature (SAT), and (c) changes in surface ocean pH in the FOSSIL-FUEL (red) and DEFOREST (orange) simulations over 1000 years of FOSSIL-FUEL and DEFOREST simulations, relative to the preindustrial state. The black dotted horizontal line represents the preindustrial state obtained by averaging over the last 100 years of the spinup simulation ZERO\_EMIS. In the DEFOREST case, atmospheric  $CO_2$ , global mean SAT, and Surface Ocean pH return close to the preindustrial levels, while they are far from the preindustrial state in the FOSSIL-FUEL case.

For delineating the contribution of snow-albedo feedback to the offset of warming from  $CO_2$  emissions in the DEFOREST case, we have performed two additional simulations: abrupt tropical (TROP\_DEFOREST) and extratropical deforestation (EXTRA\_TROP\_DEFOREST). In the TROP\_DEFOREST case, we performed abrupt deforestation in a similar manner as in DEFOREST, but between 30° N and 30° S in the first year of the model run and then allowed the vegetation to grow back in the subsequent years. In the EXTRA\_TROP\_DEFOREST simulation, we performed abrupt deforestation for regions poleward of 30° N and 30° S. In our simulations, tropical deforestation results in an emission of about 400 PgC,



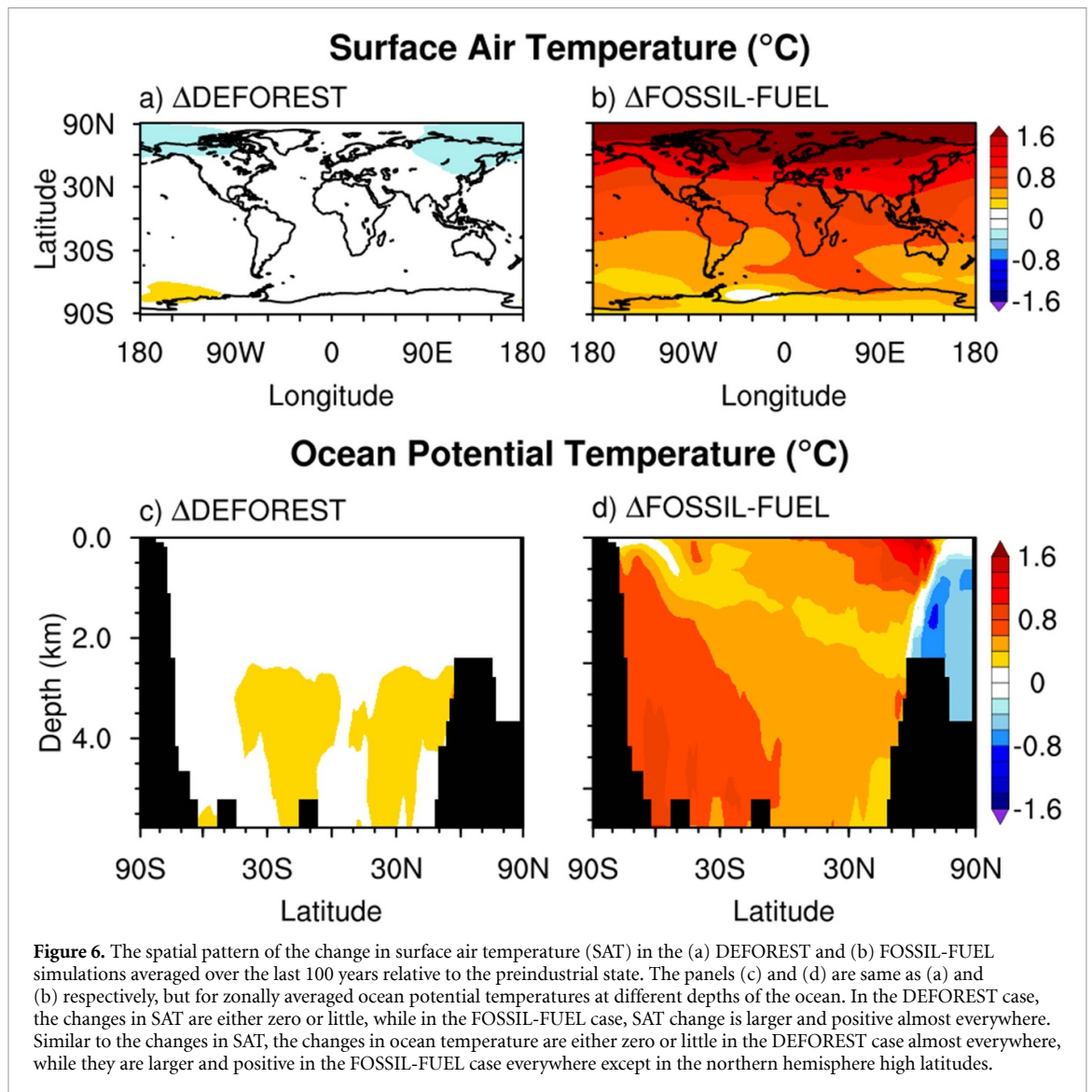


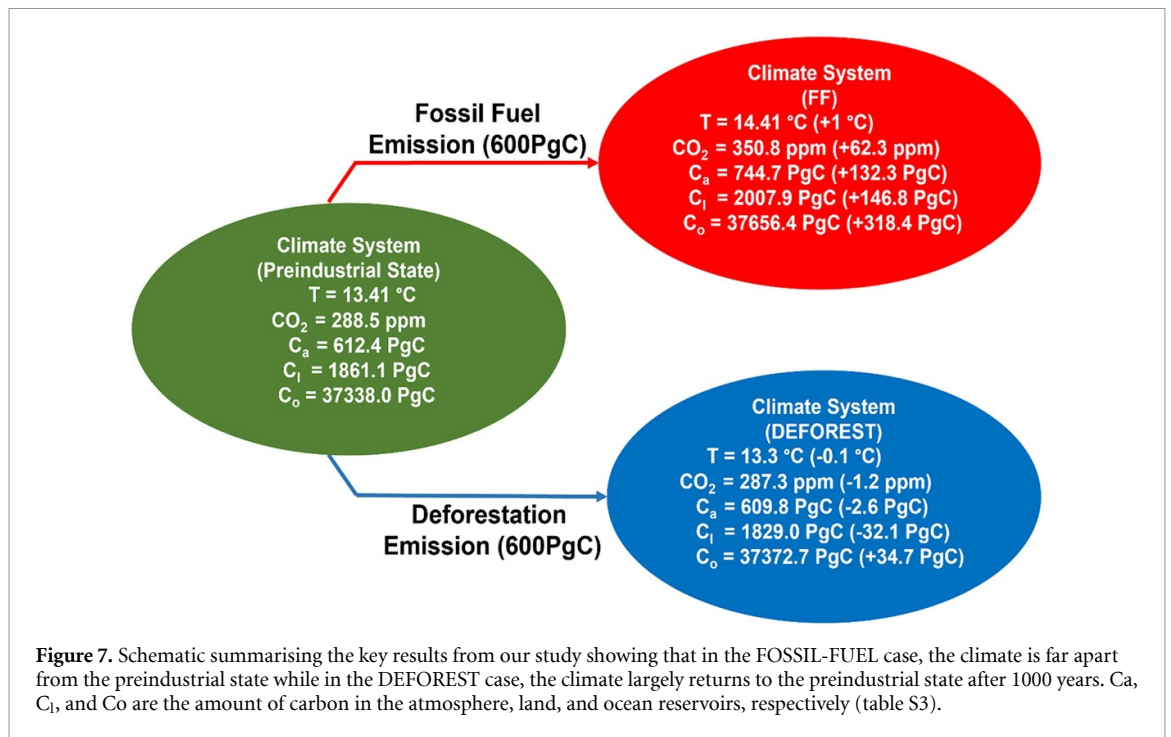
**Figure 6.** The spatial pattern of the change in surface air temperature (SAT) in the (a) DEFOREST and (b) FOSSIL-FUEL simulations averaged over the last 100 years relative to the preindustrial state. The panels (c) and (d) are same as (a) and (b) respectively, but for zonally averaged ocean potential temperatures at different depths of the ocean. In the DEFOREST case, the changes in SAT are either zero or little, while in the FOSSIL-FUEL case, SAT change is larger and positive almost everywhere. Similar to the changes in SAT, the changes in ocean temperature are either zero or little in the DEFOREST case almost everywhere, while they are larger and positive in the FOSSIL-FUEL case everywhere except in the northern hemisphere high latitudes.

whereas extratropical deforestation results in an emission of about 200 PgC. The TROP\_DEFOREST simulation results in a net warming initially, as the radiative forcing from the emitted CO<sub>2</sub> dominates the albedo effect (figure S5). However, in the EXTRA\_TROP\_DEFOREST simulation, the cooling effect from the albedo effect dominates initially, and the result is an initial cooling followed by warming when the forests grow back (figure S5). In the case of global mean SAT, the sum of tropical and extratropical deforestation responses closely follows the SAT in the DEFOREST case (figure S5), indicating the near linearity of the climate system to deforestation disturbances in latitude bands.

The spatial distribution of the difference in SAT and ocean potential temperature in the FOSSIL-FUEL and DEFOREST cases from the preindustrial state are shown in figure 6. In the FOSSIL-FUEL case, there is a large increase in SAT compared to the preindustrial state, which is more prominent in the northern hemisphere than in the southern

hemisphere (figure 6(b)). In the DEFOREST case, the changes in SAT are either zero or little in most regions (figure 6(a)). The ocean potential temperature increases in almost all the vertical layers in the FOSSIL-FUEL case, whereas the changes are either zero or little almost everywhere in the DEFOREST case (figures 6(c) and (d)).

In summary, in the DEFOREST case, the albedo change associated with our idealized deforestation disturbance partly offsets the warming from the radiative effect of emitted carbon pulse initially and the climate returns to a near preindustrial state at the end of 1000 years, while in the FOSSIL-FUEL case, the climate is warmer than the preindustrial state at the end of simulation because of additional carbon in the atmosphere. Apart from the atmospheric CO<sub>2</sub> and SAT, other parameters such as specific humidity at the surface, sea surface temperature, precipitation, evaporation, and sea ice cover also return to near preindustrial levels in the DEFOREST case, whereas they are all far from the preindustrial state in the FOSSIL-FUEL case (figure S6).



#### 4. Discussion and conclusions

Earth's near-surface carbon reservoirs can be divided into two categories, rapidly adjusting reservoirs that approach a quasi-equilibrium state on the time scale of 1000 years or less, namely atmospheric, oceanic and land-based carbon reservoirs, and slowly evolving geological reservoirs that approach a quasi-equilibrium over many thousands or even millions of years (typically sediments and the rock cycles). Emissions from the biosphere, including deforestation emissions, represent a redistribution of carbon among Earth's rapidly exchangeable surface reservoirs, whereas fossil carbon emissions represent a transfer of carbon from Earth's slowly exchangeable geological reservoirs to Earth's rapidly exchanging reservoirs.

Simulations using the UVic model indicate that about 22% of a  $\sim 600$  PgC pulse from fossil fuel emissions would remain in the atmosphere after 1000 years, producing millennial scale warming of about  $1\text{ }^{\circ}\text{C}$  and substantial amounts of ocean acidification. If the same size pulse were to be produced by a global deforestation event, with no further intervention, a spatial pattern similar to the pre-existing vegetation is projected to regrow. In this case, after 1000 years, the model predicts little change in temperature, atmospheric  $\text{CO}_2$ , or ocean temperature relative to pre-industrial state. The important results from our simulations are summarised in figure 7. Humanity in the future could choose to keep land deforested, but then the consequences would be a result of their actions, not the initial deforestation disturbance.

There are several limitations to our study. First, the simulations used in our study are highly idealized: we introduce the emissions abruptly, while in the real world, emissions are usually in pulses. However, we believe our conclusion would be unchanged if emission pulses last over the first 2–3 centuries, instead of an abrupt deforestation event in the first year, as our simulations last over a longer period of 1000 years. We have considered an unrealistic scenario of an abrupt global deforestation event to simulate a larger climate change signal. We consider the response of climate system on millennial timescales which involves several climate processes such as dynamical vegetation and deep ocean dynamics. Biophysical changes associated with deforestation such as change in surface albedo and turbulent heat fluxes lead to different climate pathways in response to same amount of carbon emissions. There are many simplifications in process representations in our simulations, and there could be uncertainty in the representation of these processes in our simulations. In the deforestation case, we do not consider the radiative forcing from associated emissions of non- $\text{CO}_2$  greenhouse gases and aerosols, which could be substantial (Ward *et al* 2014). In the real world, deforestation would result in a loss of vegetation carbon, with a part released directly into the atmosphere and the rest into the soil. The carbon that goes to the soil is released into the atmosphere through soil respiration on longer timescales. However, in our simulations, the entire carbon lost from the vegetation is released into the atmosphere instantaneously.

In our study, we consider forests that regrow immediately. However, our main conclusions would

not differ for cases where the land was maintained in a deforested state for some finite amount of time (decades to centuries). Emissions from land-use change are effectively reversible with a reverse change in the land-use. In contrast, today's fossil fuel emission will still be contributing to increased atmospheric concentrations one hundred thousand years from now (Archer 2005, Archer *et al* 2009). The simulation described above illustrate that important fundamental differences exist between fossil fuel and deforestation emissions. Absent further action (such as carbon dioxide removal and storage in geological reservoirs), a fossil-fuel CO<sub>2</sub> release is a net addition of carbon to the ocean, atmosphere and land-surface reservoir (taken collectively). In contrast, a release of CO<sub>2</sub> from the biosphere is a redistribution of carbon in that reservoir absent further action (such as continued disturbance of the land surface). Hence, previously forested land will typically recover its carbon over the centuries following the deforestation event.

### Data availability statement

The UVic Model used in our study is available free of charge from <http://terra.seos.uvic.ca/model/>. The data that support the findings of this study are available upon reasonable request from the authors.

### Acknowledgments

We acknowledge the Supercomputer Education and Research Centre, Indian Institute of Science, Bangalore, for providing the computational facility required for running the UVic model. The first author gratefully acknowledges the Prime Minister's Fellowship from the government of India. We are thankful to the developers of UVic Model for providing us with the source code of the model. We are also thankful to Dr Michael Eby (School of Earth and Ocean Sciences, University of Victoria, Canada), and Xiaoyu Jin (Dept. of Atmospheric Sciences, School of Earth Sciences, Zhejiang University, China) for helping us with instructions for running the simulations.

### Author contributions


Ken Caldeira, Govindasamy Bala and Long Cao formulated the idea behind the study. Govindasamy Bala, K U Jayakrishnan and Ken Caldeira designed the experiments. K U Jayakrishnan performed the experiments with support from Long Cao. All the authors contributed to writing and editing of the manuscript.

### ORCID iDs

K U Jayakrishnan  <https://orcid.org/0000-0001-5518-2356>

Govindasamy Bala  <https://orcid.org/0000-0002-3079-0600>

Long Cao  <https://orcid.org/0000-0002-8336-4242>

Ken Caldeira  <https://orcid.org/0000-0002-4591-643X>

### References

- Archer D 2005 Fate of fossil fuel CO<sub>2</sub> in geologic time *J. Geophys. Res. C: Oceans* **110** 1–6
- Archer D *et al* 2009 Atmospheric lifetime of fossil fuel carbon dioxide *Annu. Rev. Earth Planet. Sci.* **37** 117–34
- Bala G, Caldeira K, Wickett M, Phillips T J, Lobell D B, Delire C and Mirin A 2007 Combined climate and carbon-cycle effects of large-scale deforestation *Proc. Natl Acad. Sci. USA* **104** 6550–5
- Bathiany S, Claussen M, Brovkin V, Raddatz T and Gayler V 2010 Combined biogeophysical and biogeochemical effects of large-scale forest cover changes in the MPI earth system model *Biogeosciences* **7** 1383–99
- Boysen L R *et al* 2020 Global climate response to idealized deforestation in CMIP6 models *Biogeosciences* **17** 5615–38
- Ciais P *et al* 2013 Carbon and other biogeochemical cycles. Climate change 2013: the physical science basis *Contribution of Working Group I to the Fifth Assessment Report of the Intergovernmental Panel on Climate Change (IPCC)* vol 18 pp 95–123
- Claussen M *et al* 2002 Earth system models of intermediate complexity: closing the gap in the spectrum of climate system models *Clim. Dyn.* **18** 579–86
- Davin E L and de Noblet-ducoustre N 2010 Climatic impact of global-scale Deforestation: radiative versus nonradiative processes *J. Clim.* **23** 97–112
- Devaraju N *et al* 2018 Quantifying the relative importance of direct and indirect biophysical effects of deforestation on surface temperature and teleconnections *J. Clim. Appl. Meteorol.* **31** 3811–29
- Devaraju N, Bala G and Nemani R 2015 Modelling the influence of land-use changes on biophysical and biochemical interactions at regional and global scales *Plant Cell Environ.* **38** 1931–46
- Eby M, Zickfeld K, Montenegro A, Archer D, Meissner K J and Weaver A J 2009 Lifetime of anthropogenic climate change: millennial time scales of potential CO<sub>2</sub> and surface temperature perturbations *J. Clim.* **22** 2501–11
- Eyring V, Bony S, Meehl G A, Senior C A, Stevens B, Stouffer R J and Taylor K E 2016 Overview of the Coupled Model Intercomparison Project Phase 6 (CMIP6) experimental design and organization *Geosci. Model Dev.* **9** 1937–58
- Friedlingstein P *et al* 2020 Global carbon budget 2020 *Earth Syst. Sci. Data* **12** 3269–340
- Govindasamy B, Duffy P B and Caldeira K 2001 Land use changes and Northern Hemisphere cooling *Geophys. Res. Lett.* **28** 291–4
- Houghton R A 2007 Balancing the global carbon budget *Annu. Rev. Earth Planet. Sci.* **35** 313–47
- Keller D P, Oeschles A and Eby M 2012 A new marine ecosystem model for the University of Victoria earth system climate model *Geosci. Model Dev.* **5** 1195–220
- Kravitz B *et al* 2015 The Geoengineering Model Intercomparison Project Phase 6 (GeoMIP6): simulation design and preliminary results *Geosci. Model Dev.* **8** 3379–92

- Lawrence D M *et al* 2016 The Land Use Model Intercomparison Project (LUMIP) contribution to CMIP6: rationale and experimental design *Geosci. Model Dev.* **9** 2973–98
- Le Quéré C *et al* 2009 Trends in the sources and sinks of carbon dioxide *Nat. Geosci.* **2** 831–6
- Lean J and Rowntree P R 1993 A GCM simulation of the impact of Amazonian deforestation on climate using an improved canopy representation *Q. J. R. Meteorol. Soc.* **22** 509–30
- Mathesius S, Hofmann M, Caldeira K and Schellnhuber H J 2015 Long-term response of oceans to CO<sub>2</sub> removal from the atmosphere *Nat. Clim. Change* **5** 1107–13
- Meissner K J, Weaver A J, Matthews H D and Cox P M 2003 The role of land surface dynamics in glacial inception: a study with the UVic Earth System Model *Clim. Dyn.* **21** 515–37
- Montenegro A, Brovkin V, Eby M, Archer D and Weaver A J 2007 Long term fate of anthropogenic carbon *Geophys. Res. Lett.* **34** 1–5
- Petäjä T *et al* 2021 Influence of biogenic emissions from boreal forests on aerosol–cloud interactions *Nat. Geosci.* **15** 42–47
- Simmons C T and Matthews H D 2016 Assessing the implications of human land-use change for the transient climate response to cumulative carbon emissions *Environ. Res. Lett.* **11** 035001
- Skvortsov A, Eby M and Weaver A 2009 Snow cover validation and sensitivity to CO<sub>2</sub> in the UVic ESCM *Atmos. Ocean* **47** 224–37
- Snyder P K, Delire C and Foley J A 2004 Evaluating the influence of different vegetation biomes on the global climate *Clim. Dyn.* **23** 279–302
- Spracklen D V, Bonn B and Carslaw K S 2008 Boreal forests, aerosols and the impacts on clouds and climate *Phil. Trans. R. Soc. A* **366** 4613–26
- Tölle M H, Engler S and Panitz H-J 2017 Impact of abrupt land cover changes by tropical deforestation on Southeast Asian climate and agriculture *J. Clim.* **30** 2587–600
- Ward D S, Mahowald N M and Kloster S 2014 Potential climate forcing of land use and land cover change *Atmos. Chem. Phys.* **14** 12701–24
- Weaver A J *et al* 2001 The UVic earth system climate model: model description, climatology, and applications to past, present and future climates *Atmos. Ocean* **39** 361–428